Aciaria / Steelmaking
ISSN 1982-9345
43º Seminário de Aciaria – Internacional / 43rd Steelmaking Seminar – International

SECONDARY SYSTEM MECHANICAL RESONANCE IN NEW TALL-SHELL SDI-BUTLER ARC FURNACES: DETECTION AND SOLUTIONS[1]

Ron E. Gerhan[2]
Yury Krotov[3]
Nicolás Lugo[2]

Abstract
In an effort to develop high productivity, energy efficient, scrap-flexible furnaces, an EAF trend is moving to larger, typically single charge, furnaces. One solution, implemented in a number of plants, is to increase the height of the EAF shells. New, taller shell configurations and increased electrode column length present a challenging situation for graphite electrodes in the EAF. Along with the increased bending moment below the electrode holder, some furnaces exhibit the phenomenon of high energy electrode vibrations potentially leading to electrode breakage. We present vibration analyses results and techniques to reduce the impact on electrode vibration.
Key words: Electrodes; Resonance; Natural frequency.

[1] *Technical contribution to the 43nd Steelmaking Seminar, May, 20th-23rd, 2012, Belo Horizonte, MG, Brazil.*
[2] *GrafTech International Holdings Inc., 12900 Snow Road, Parma, Ohio 44130; nicolas.lugo@graftech.com.*
[3] *Dr., Steel Dynamics, Inc., Structural and Rail Division, 2601 South Country Road 700 East Columbia City, Indiana 46725.*

1 INTRODUCTION

In a continuous effort for improvements in efficiency and productivity, Arc Furnace (EAF) technology has developed a new generation of designs and capacities. These developments made it possible for this 110 years old technology to secure a place in today's steelmaking. The modern EAF operations combine high electrical and chemical energy input with minimal power-off time.
In the latter part of 1990's, furnace manufacturers started increasing shell height in order to reduce number of scrap charges, reduce tap-to-tap time and improve overall process productivity. In certain cases the move to taller shells dramatically increased electrode breakage, due to an increase in scrap cave severity and high energy electrode oscillation. A longer electrode column leads to a greater risk of exciting violent mechanical mast-arm-electrode oscillation. This type of oscillation will be further referred to as simply electrode vibration.

2 DISCUSSION

The intention of this work is to explain the phenomenon of electrode vibration, introduce GrafTech's new electrode vibration analysis system, and explain efforts undertaken by Steel Dynamics and GrafTech. These efforts resulted in minimizing electrode vibrations, improving power input rate and reducing the rate of electrode breaks in SDI's revamped, taller, single charge furnaces.
Some advantages of taller, single charge EAF designs are the following:

- no lost production time due to additional roof openings for the second charge;
- no lost energy due to roof openings;
- improved energy efficiency due to single bore-in, earlier foaming, and better arc stability;
- improved oxygen energy yield because of more efficient post-combustion;
- improved burner efficiency for scrap melting.

Taller furnaces combine operational and maintenance advantages of standard AC furnaces yet with some energy recovery features of furnaces with scrap preheating. In the last decade new taller EAF designs were successfully implemented in USA and Europe.(1)
Some of the disadvantages of taller, single charge EAF designs are:

- higher heat losses due to larger water cooled panel area;
- higher rate of electrode breaks due to more sever scrap cave-ins, electrode vibration and higher mechanical stresses.

An important factor affecting electrode vibration is a pitch circle diameter (PCD). The effect of PCD on electrode column-mast-arm resonance was realized during the 1980's. At a time when refractory erosion was posing a significant threat to the furnace walls, furnace manufacturers reduced PCD in an effort to minimize the deleterious effect the arcs exerted on the refractory and water cooled panels. The combination of low reactance, tight PCD and strong primary power systems led to an increase of electromagnetic forces, especially during the melting stage.
Larger electromagnetic forces produce increased mechanical stresses on the secondary system structure. If left uncontrolled, these forces may excite the electrode column-mast-arm's natural frequency resulting in high amplitude steady oscillation (electrode vibration). This type of oscillation results in large mechanical stresses on the electrode column and, eventually, electrode breaks.

The phenomenon of electrode vibrations in the AC EAF secondary system has been discussed for an extended period of time. For example, in the 1970's the largest EAF in the world experienced this type of problem.[2] After several attempts to solve a severe breakage problem that appeared after the EAF revamp, a solution was finally achieved by increasing the electrode diameter from 600 mm to 700 mm. This was the first facility in the world to use 700 mm electrodes.
Ehle *et al*.[3] presented solutions to a unique case of excessive electrode breaks on a 360 tonne furnace after the implementation of current conducting arms. In that same time period, Maduell and Bowman[4] described a successful solution to resonant vibrations causing poor electrical performance in a low reactance furnace.

2.1 Magnetic Forces as the Cause of Vibrations in the Secondary System

The magnetic fields created by the constantly changing currents in an electric arc furnace have a significant impact on the furnace's overall mechanical performance. These fields are responsible for "pushing" the electric arcs away from each other in an AC furnace, erratic cable movement during the bore-in and melting stages, as well as some of the arc deflection problems in DC furnaces.[5] Occasionally, the magnetic field effect phenomenon presents a challenge to EAF manufacturers and operators. The new trend in furnace design of taller EAF shells, makes this issue even more significant, since longer electrode columns are easier to excite into their natural resonant frequencies.
The magnetic force (Lorenz force), *f*, per unit length between two conductors is proportional to the product of their currents, *I*, and inversely proportional to the distance between conductors, *d*. The force is positive, (attraction), for currents in the same direction and negative, (repulsion), for opposite currents.[6]

$$f = \frac{\mu_0 I_1 I_2}{2\pi d} \qquad (1)$$

In AC furnaces the electromagnetic force acting on one electrode is a function of all three currents. Electromagnetic forces present in the EAF along the components of the secondary system present a very complex pattern. Figure 1 displays a plan view of forces acting on the electrodes. As explained by several authors these forces tend to push the AC arcs in the direction familiar to all, towards the EAF hot spots. Given the fact that the holders on the outer phases move more easily side-to-side, the only force being considered here on A and C phases are in the X direction. Below is the calculation of the force exerted on C phase.[7] The force has magnitude of N/m if currents are in kA and PCD is in meters.

$$F_c(X) = \frac{10^{-1}}{PCD}\left(\frac{1}{\sqrt{3}}\right)\left[3i_c^2 + i_a^2 - i_b^2\right] \qquad (2)$$

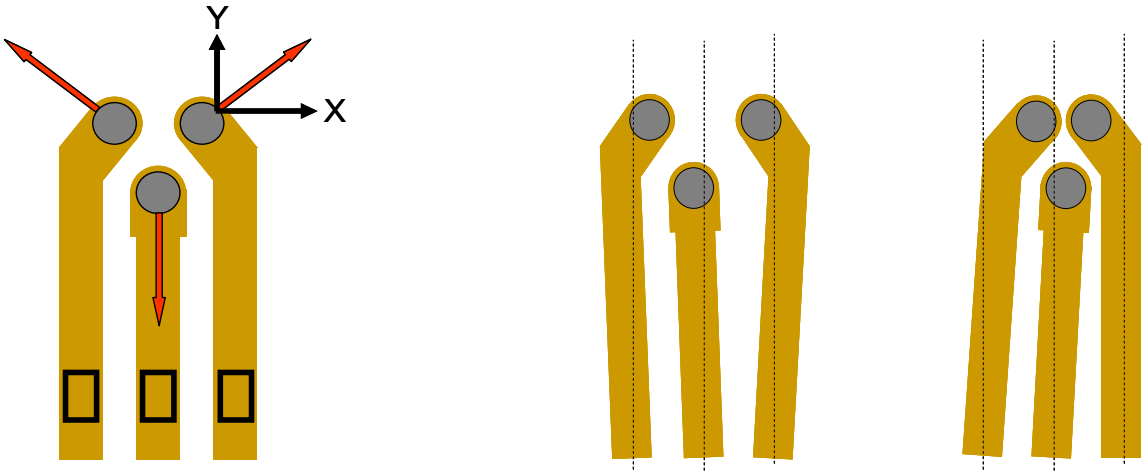

Figure 1. Forces acting on electrodes (left), resulting coupled motion, (right).

For the center phase, the major force component is directed in line with its arm (Y direction), therefore the motion tends to occur in the electrode column only since the mast arm assembly is much stiffer in this direction:

$$F_b(Y) = -\frac{10^{-1}}{PCD}\left[2i_b^2\right] \tag{3}$$

The center phase suffers magnetic forces in the X direction only when the outer phase currents are unbalanced:[7]

$$F_b(X) = \frac{10^{-1}}{PCD}\frac{2}{\sqrt{3}PCD}\left(i_a^2 - i_c^2\right) \tag{4}$$

These equations apply to the forces exerted on triangulated electrodes. There are also forces exerted on the arms but these tend to have a lower impact since the moment is lower than that for the electrodes. Forces on the cables are assumed not to act on the arm.

There are multiple vibration modes in the EAF system[3] but the easiest to detect visually (and aurally) in a three phase AC furnace is the simultaneous outwards/inwards swings of the outer phases coupled with a phase displaced swing of the center phase (Figure 1). A and C phase mechanical oscillations have 180 degrees phase shift while B phase is observed to have an approximate 90 degrees or 270 degrees phase shift with respect to A or C phase. Such a coupled motion was also deduced from recent detailed modeling by Brusa, Franceschinis and Mersut.[8]

Forces on the electrodes in line with the arms, (Y direction), are acting within a generally stiffer mechanical system of the mast arm and tend to be of higher frequency. In particular the center phase, normally shorter and therefore the stiffest, has a tendency to restrict the motion mainly to the electrode column. The result is often a higher frequency, in the 4 Hz to 6 Hz range, depending on the length of the electrode column.

The initiation of prolonged resonant swings of the secondary system begins with the contact of an electrode with the inside of the electrode bore pit. The subsequent high current surge throws the phase outwards. It then swings back inwards such that repetitive contacts occur, as demonstrated by the arc voltage measurements of Remus[10] and discussed by Bowman and Krüger.[7] Due to the current coupling

ISSN 1982-9345

between phases, the phase electrically ahead also experiences a large electromagnetic force and therefore also moves away. Once two phases are set into resonance (usually the outers) it is very probable that the third will follow.
The longer columns associated with taller shells have led to a reduction in the typical natural frequency of the furnaces secondary system. In recent studies, we have measured resonant frequencies lower than those quoted above. Another situation present with lower resonance frequencies is larger effective tip displacement. Larger displacement translates into greater bending forces on the electrode below the holder. Greater forces impose greater mechanical stresses on the electrodes.

2.2 Resonance Resulting in Electrode Break

Figure 2 presents an example of current records demonstrating a resonant condition at 2.4 Hz. After approximately 30 seconds of continuous resonance C phase electrode, bottom plot, broke.

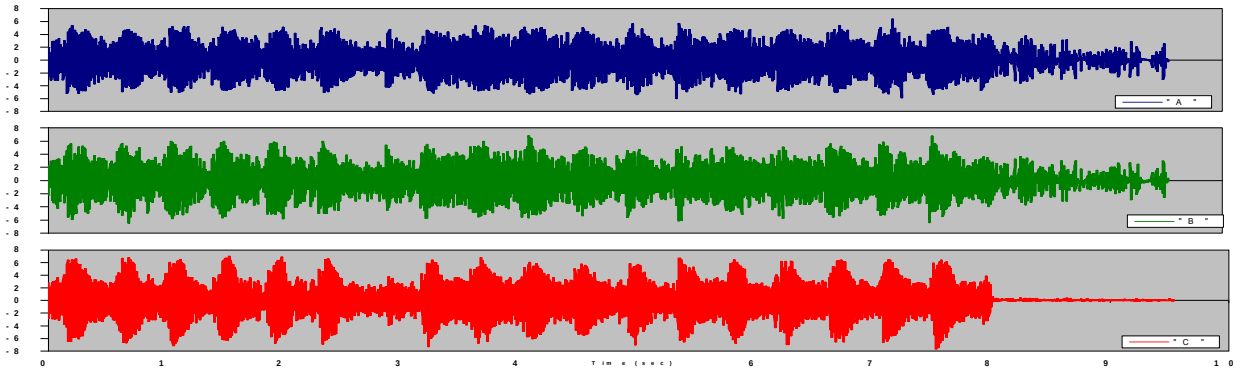

Figure 2. Primary currents before electrode break on C phase.

Appling the above C phase currents to Equation 2, the resulting X direction, or outward, forces which lead to the electrode break can be calculated. Figure 3 shows these magnetic forces, calculated in Newtons per unit length, consistently reached 4,000 N/m. Table 1 summarizes peak forces on the three phases for the above current conditions.

Table 1. Estimated peak forces

Phase	Direction	Peak force, N/m
A	-X	2,600
B	**-Y**	**2,000**
C	X	4,000

For all three phases, the peak force in the perpendicular directions reached similar levels, and in all cases the minimum force was approximately 300 N/m to 500 N/m. Our analysis of the circuit shows that C phase was suffering repetitive short circuits before the break. Peak current on C phase was about 120 kA rms. Peak force over the 7 m length of the column of C phase reached about 2.85 tonne.

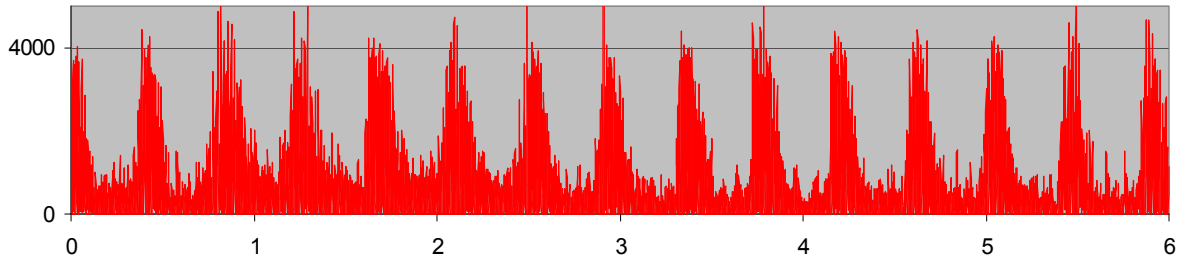

Figure 3. Forces in the X direction on C phase (N/m).

2.3 Stresses on the Electrode Column

The natural frequency of a phase of the secondary system depends on the mechanical properties of its components, principally the length and stiffness of the mast, arm and electrode. The highest stress on the electrode column occurs when the vibration mode is at the lowest frequency since this corresponds to the largest amplitude of the swing. Generally this is the mode where the mast, arm and electrode move together to obtain the largest deflection. The mast and arm can both twist and bend while the electrode only bends. The longer and 'softer' the components are, the larger the amplitude for a given force.
Resonant amplitude depends on the system damping and the driving force. The major part of the damping occurs within the graphite electrode due to its non-linear stress/strain characteristic. Our modeling of this case shown above, estimates the electrode tip is swinging through an arc of +/- 40 mm if the electrode length below the holder is 7 m. Of this amount, approximately +/- 17 mm of swing is due to the bending of the electrode column. Such bending is close to the limit that a joint just below the holder can withstand before breaking.

2.4 The GrafTech Portable Electric Arc Furnace Analyzer (PAFA)

Features of the GrafTech Phoenix™ PAFA have been previously presented.[9] However, it is important to reiterate that PAFA features include: open architecture, high speed data sampling and simultaneous multiple channel input, thus enabling Graftech to further develop furnace analysis techniques for the ever-changing electric arc furnace operation. As a result of GrafTech's involvement as technical support to Steel Dynamics, (Butler, Indiana), the new electrode vibration analysis module was developed and incorporated into the many Customer Technical Service Tools offered by GrafTech International.

2.5 PAFA Electrode Vibration Module

One of the most commonly accepted methods of depicting furnace performance is via trend charts. Trend charts, whether displaying current, voltage, or Megawatts easily show when in a heat events occur. If good electrical transducers are used for data collection, one second sampling rates are sufficient. At this rate, the data file for an average heat contains about 2,500 data points per channel. The chart shown in Figure 4 displays nine variables and is probably the most basic of trend charts.

ISSN 1982-9345

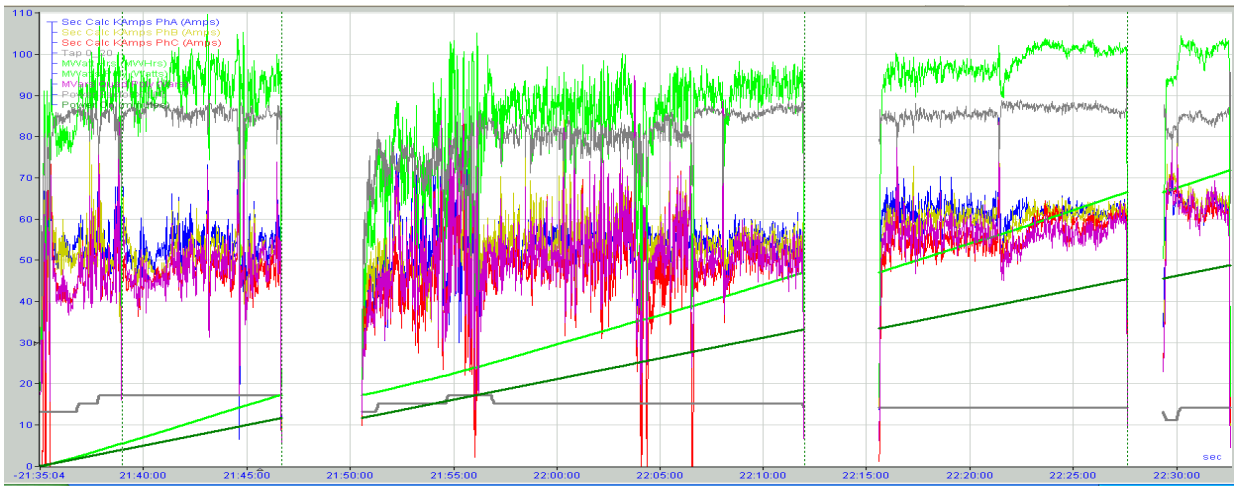

Figure 4. Heat trend-charts.

Traditional arc furnace analysis uses one secondary trend charts extensively for furnace analysis; a closer look sometimes yields interesting results. For simplicity, one channel demonstrating secondary A-phase current will be discussed.

The two trend charts displayed in Figure 5 both show secondary current for phase-A. The left chart uses the traditional one second RMS value while the right chart uses a RMS value calculated over a significantly shorter time period. It can be clearly seen from these charts the smoothing effect of one second data, i.e. the maximum one second current level displayed is 85 kA, while the maximum current level is for the significantly shorter time period is 98 kA. As the time period shortens, greater current variations are detected. While it is highly unlikely furnace control can be effectively achieved for detected currents changing faster than once a second, the changing currents do produce the aforementioned magnetic and mechanical forces

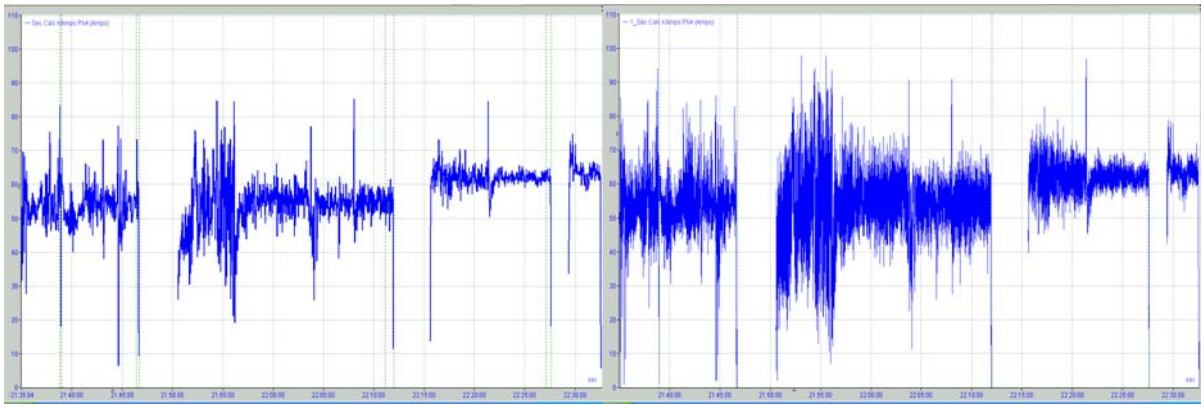

Figure 5. Smoothing effects of one second rms current values.

Traditional vibration analysis utilizes concept of Fourier transformation. This type of analysis requires large amounts of data and data-processing capability. A more common version is the Fast Fourier transformation (FFT). FFT analysis is highly effective at detecting oscillations and their associated harmonics, but still requires substantial amounts of data and processing efforts, especially at high frequencies and high data sampling rates.

To find oscillation on a 50 Hz or 60 Hz carrier wave, data sampling rates must be significantly fast. The GrafTech Phoenix System has a base sampling rate in the millisecond range and can support oscillation detection of several harmonics. Figure 6 shows an current example of the millisecond base sampling data, (blue),

The traditionally calculated one second RMS values, (green), and the significantly faster calculated RMS values, (red**).**

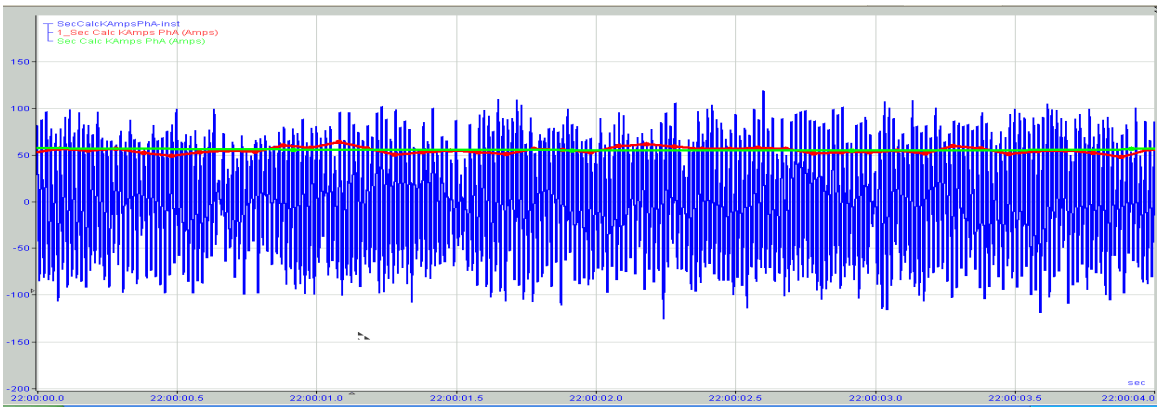

Figure 6. One second current value.

To achieve a discerning resolution, several thousand millisecond data samples are used in every FFT calculation. These samples represent a few seconds of furnace operation, which is sufficient to detect operational changes.

When applying an FFT to such data as described above, distinct frequencies become apparent, top chart in Figure 7. The main carrier 60 Hertz wave is the dominant frequency. Also appearing as sidebands are frequencies at 56.2 Hertz and 63.8 Hertz. The presence of the two equidistant sidebands confirms a vibration frequency of 3.8 Hz. The processing of this FFT is fairly complex and best completed during off-line analysis.

GrafTech has developed a proprietary online analysis technique which not only specifies the frequency of a vibration when present, but also assigns a magnitude to it. The top graph in Figure 7 is the FFT as described above. The second and third graphs, respectively, show the frequency and magnitude of the vibration as determined by GrafTech's proprietary real-time electrode vibration analysis. The bottom graph shows where in the heat the vibration analysis was performed.

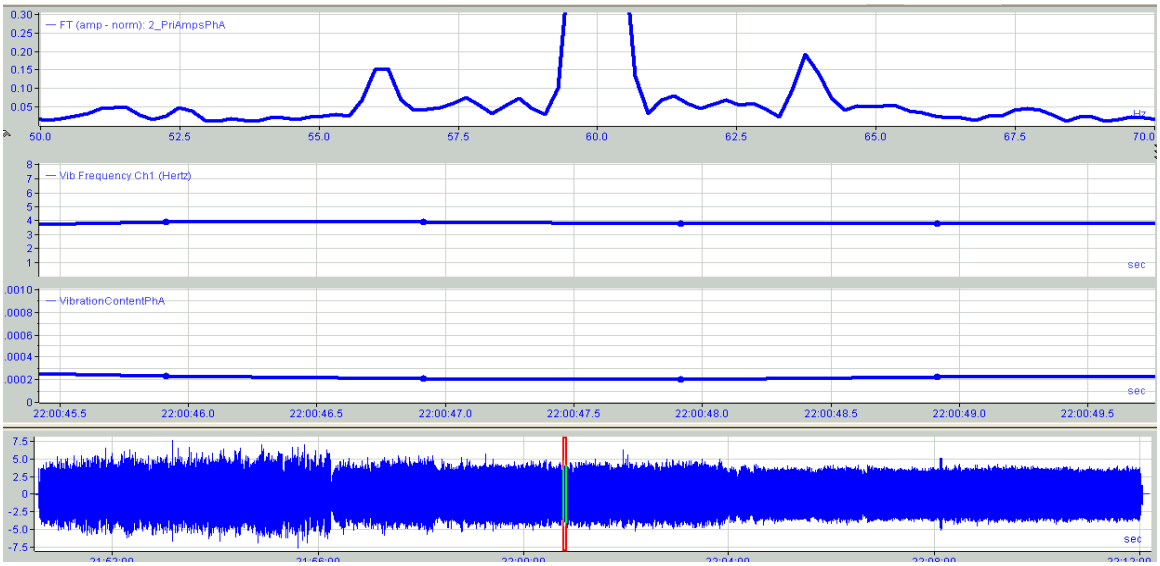

Figure 7. Vibration frequency and magnitude.

Figure 8 demonstrates the vibration frequencies and magnitude for approximately 20 minutes of scrap melting. The light blue green line is the magnitude and the dark

blue is the frequency. Both values are calculated every second with the magnitude being an accumulated value. As can be seen, the detected frequencies do fluctuate, but steady periods of vibration are apparent. The vibrations are “strongest” where the slope of the magnitude trend is the steepest. Therefore, to get a complete analysis, the magnitude of the vibration must be considered along with the frequency.

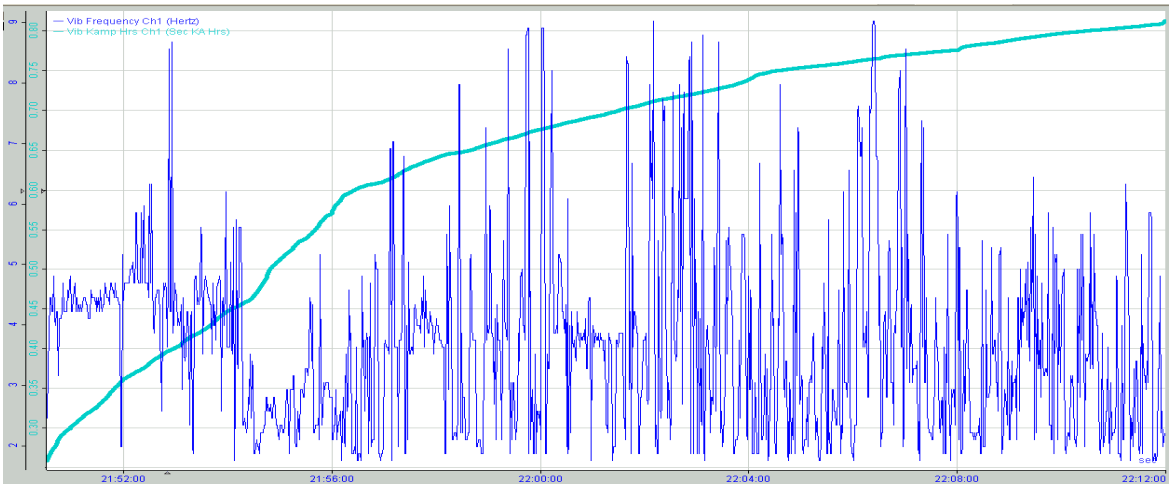

Figure 8. Dominant frequency (blue) and accumulated magnitude (blue green).

Further histogram analysis can determine the dominant mode frequencies as well as the associated magnitudes (Figure 9). The two dominant mode frequencies are 1.8 hertz and 3.8 hertz. The two frequencies with maximum magnitude are 2.3 hertz and 4.4 hertz.

Vibration frequencies can be grouped into 3 categories. Vibrations below 2 Hz depict a vertical electrode movement and are caused by up/down mast motion and regulator control. Vibrations between 2 Hz and 5 Hz are caused by system’s horizontal motion, and vibrations above 5 Hz are caused by a pendulum motion of the electrode tip. The actual boundaries of vibration frequencies i.e. 2 Hz, 5 Hz, are approximate and will vary according to structural characteristics of each furnace.

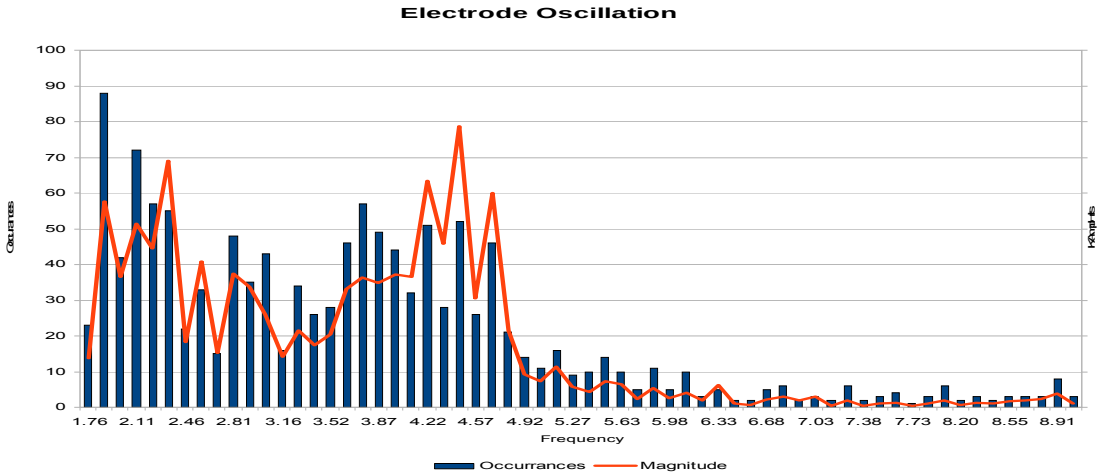

Figure 9. Histogram of occurrences and magnitude as a function of frequency.

The new electrode vibration module in the Portable Electric Arc Furnace Analyzer (Phoenix-PAFA) now allows for quantifying the severity of electrode vibrations. The

magnitude and frequency are quantified for each phase, such that they can be used with all other furnace parameters either graphically or in tabular form.

2.6 The SDI Case

Steel Dynamics Inc. at Butler, Indiana is a flat-rolled mini mill currently operating two twin shell furnaces; two SMS thin slab casters, a seven-stand rolling mill and cold rolling and finishing facilities. The plant started operations in 1995 with one twin-shell Fuchs furnace ('Battery 1') and one caster. In 1997 a second twin-shell ('Battery 2') and a second caster were commissioned. Both furnaces are powered by 120 MVA transformers that were running at approximately 100 MW levels with melting capacity of 2.7 million short tons per year (MTPY) before the furnace upgrade. SDI utilizes various grades of scrap and hot metal (about 10% of the charge weight) produced by Iron Dynamics.

As part of plant production increase plan (3 MTPY), the volume of the furnaces was increased to accommodate all the scrap in a single roof opening. The goal was to reduce power-off time and energy losses, and to increase power input rate by avoiding a second bore- in.

Due to geometrical constraints the furnace diameter remained unchanged. The only way to increase furnace volume was to increase its height, in this case by 1.5 m. This increase in furnace height required an increase in electrode column length up to 7 m below the holder.

Before the modifications took place, the length of a new electrode column was approximately 8.1 m or 3 full (2,700 mm) electrodes. The average length below the holder was 5.6 m, approximately. With this configuration, the EAFs did not show any sign of mechanical resonance that resulted in electrode breaks or mechanical maintenance issues.

Upon completing Battery 1 upgrade, severe electrode vibrations occurred resulting in an increase of high column electrode breaks. The predominant vibration mode was between the outer phases (A and C) with the frequency ranging from 2.1 Hz to 2.6 Hz. This situation was especially critical during the early part of the heat, from beginning of bore-in to approximately 20 MWh into the melting process. In some extreme cases, resonant conditions were also detected on flat bath (Figure 10).

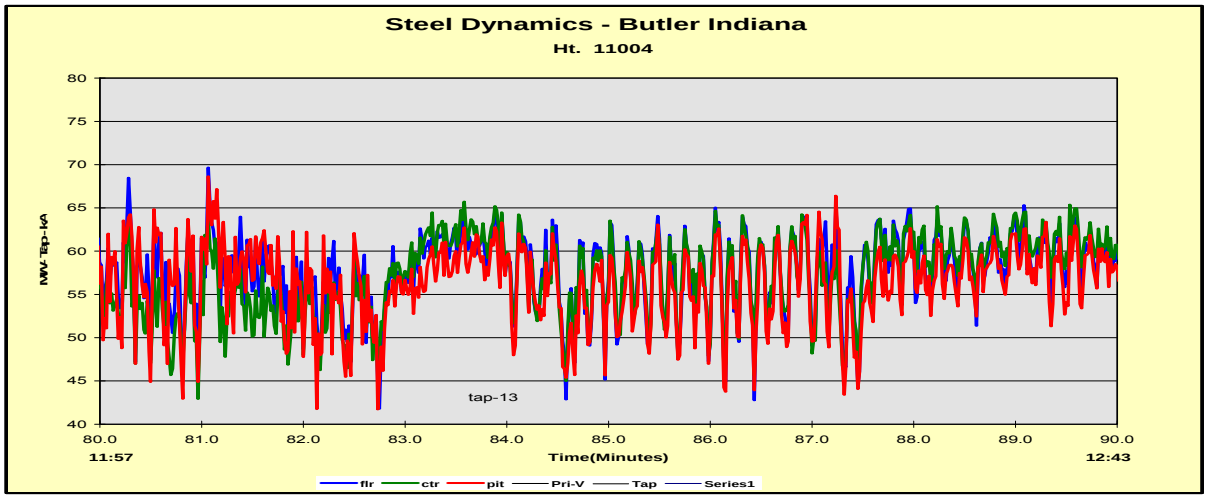

Figure 10. Current trend line demonstrating a resonant condition in flat bath.

SDI had anticipated possible technical challenges in operation with longer electrode columns. At SDI's request GrafTech ran proprietary electrode performance models of a long column operation. Obviously, these models predicted a sizable increase on electrode breakage. Even though, SDI realized the productivity gains were worth whatever EAF modifications necessary to minimize the negative effects associated with the increase in column length.
The furnace upgrade initially did not include changes to any furnace controls. Therefore during startup, the furnace was controlled as though it still had smaller shells. As mentioned in the previous section, the electrode columns started oscillating sideways as soon as the outer electrodes touched the scrap. Upon realizing the severity of the situation, several scenarios and solutions were proposed and executed. These changes involved modifications in the operational, mechanical, electrical and electronic components of the system. Each of the steps taken added to the final solution. Team member experience and available information research was crucial to the evaluation and execution of each progressive step. The major steps taken are outlined below.

3 CONCLUSIONS

3.1 Scrap Make-Up

During the first few heats after start-up it was observed that the column vibrations were the strongest with dense, hard-to-melt scrap high in the furnace. At this time the practice for scrap loading was changed. Loading the furnace is still carried out with two buckets, back-to-back before power-on, using only light scrap in the second bucket, i.e. bushelings and shredded. All the heavy, dense scrap is loaded in the first bucket, with hot metal from the Iron Dynamics plant poured on top.

3.2 Power Program, Long Arcs and Arc Stability

Investigation of the first electrode break revealed three small pits instead of the previous single larger bore down pit. The clearance between the electrodes and the un-melted scrap was unusually small. To increase the distance between the electrode and the solid scrap the power program was set to go to the highest arc voltage available (over 600 V) as soon as practically possible. Knowing that powerful arcs will cut through shredded scrap with little difficulty, reduction of the bore-down speed was also implemented.
The practice implemented is - start arcing on Tap-13 (1,200 V) to protect the roof, switching to Tap-15 (1,280 V) as soon as possible. After four MWh Tap-17 (1,350 V) is used for the rest of the melting stage. This could be considered a very aggressive melting practice. However, the first roof delta lasted over 1,200 heats.
The average power per heat ranged from 94 MW to 100 MW, depending on the "smoothness" of the melting profile (arc stability). It was also observed that the regulator's ability to maintain the operating set-point early in the heat was far more difficult when the water cooling rings (WCR) were on (Figure 11). The practice of delaying the WCR until 6 MWh into the heat was implemented. After this change, most of the arc instability associated with excess water early in the heat was eliminated.

ISSN 1982-9345

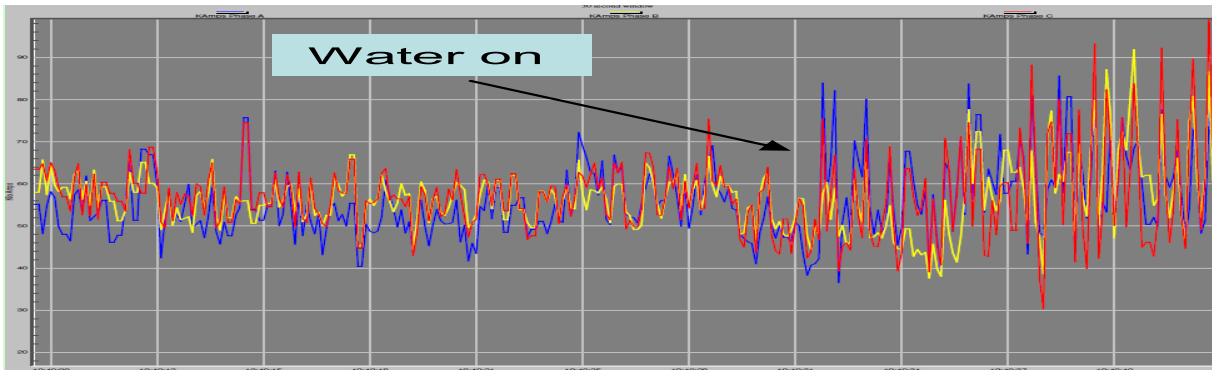

Figure 11. Effect of electrode cooling water on arc stability.

3.3 Regulation Adjustments

SDI furnaces are equipped with supplementary reactors (up to 2.5 Ω at 34.5 kV). This allowed for very aggressive power input levels with the option to operate the transformer up to 1,350 V phase to phase. Taking advantage of the reactor's smoothing characteristics SDI furnaces were set to run at "very high" regulation speeds during the main melting stage. Aggressive down speeds and approximately 20% more electrode mass produced an overshooting effect in the down direction. Regulator reaction to the high current spikes produced a continuous cyclical side to side and up - down electrode motion.
Although several regulation adjustments were made, the resulting reduction in down speed had the greatest impact. The final effective reduction in down speed was 50%. This corrective action, although helpful did not fully eliminate the breakage situation, especially when heavy scrap, high in the furnaces, was present.

3.4 Increased Reactance

As stated above, the maximum supplementary reactance value of this system is 2.5 Ω. This air core type reactor is equipped with five taps (2.5 Ω down to 1 Ω). The reactor was set to 2.1 Ω before the upgrade. After the initial attempt to run on this setting, a decision was made to increase the reactor settings to 2.5 Ω, since the phenomenon of mechanical resonance and related electrode breaks were still present.
The increase in reactance further reduced the number of heats in which mechanical resonance was detected. However sporadic electrode breakage was still present, presumably caused by higher percentage of bundles and scrap falling from higher off the furnace wall.

3.5 Stronger Electrode Joint

A possible previous solution to scrap-cave related breaks was to strengthen the electrode column by increasing electrode diameter. SDI did not consider this solution since this would add considerable weight to the electrode column in a system designed for 600 mm electrodes. They alternatively decided to try a special electrode joint involving a larger diameter connecting pin. The result of using this stronger joint system was a measurable reduction in the frequency of electrode breaks. The main disadvantage is that it would be a non standard electrode joint.

3.6 Increase in Electrode Pitch Circle (PCD)

The main goal was to reduce the repulsive magnetic forces by increasing the distance between the electrodes, since forces are inversely proportional to the distance. Accordingly the PCD was increased from 1.25 m to 1.33 m, the maximum distance allowed without requiring electrode arm modifications.

Acknowledgements

We would like to thank Ricky Rollins, Tim Bosserman, Bob LaRoy, Bryan Butcher and the meltshop/maintenance personnel at SDI for their support and participation, Ben Bowman for his support in the writing of this paper and Said Alameddine of Graftech for his participation in the development on the Electrode Vibration Module.

REFERENCES

1 S. Laurenti, R. Gottardi, S. Miani and A. Partyka, “High performance single-bucket charging EAF practice” Iron and Steelmaking 2005, vol. 32
2 W. Schwabe and P. Robinson “Characteristics of high productivity arc furnaces for steel production” Proceedings of the Third International Iron and Steel Congress 16-20 April 1978, Chicago, Illinois, Materials Park, OH: ASM International, 1979 Pages 291-295
3 J. Ehle, K. Timm, B. Remus and H. Knapp, “Vibrational analysis and first operational results of current conductive electrode arms on 400 t-arc furnaces”, electrowarme international 50 (1992)
4 F. Maduell and B. Bowman, “Effect of adding reactance on furnace performance at CELSA” , 4th European Electric Steel Congress, Madrid, 1992, p. 203-213F
5 B. Bowman and N. Lugo, “Arc deflection in various designs of EAF” Millennium Steel 2001 pages 172-174
6 E. M. Purcell, *Electricity and Magnetism*, London, McGraw-Hill Science, 1984.
7 B. Bowman and K. Krüger, *Arc Furnace Physics* , Verlag Stahleisen 2009, p 176-190
8 E. Brusa, E. Franceschinis and S. Mersut, “Compact modeling of electric arc furnace electrodes for vibration analysis, detection and suppression”, CMES, vol 42, no. 2, 2009, p 75-106.
9 B. Remus, “Analyse elektromechanischer Schwingungen von Elektroden-Tragarm-System an Drehstrom-Lichtbogenöfen” (*Analysis of the electromechanical swings of the electrode-arm system on AC arc furnaces*). Dr.-Ing. Thesis, University of the Federal Armed Forces, Hamburg, 1984

BIBLIOGRAPHY

1 R. Gerhan and N. Lugo “Achieving the optimum melting power in the EAF and the use of GrafTech special EAF monitoring system” XXXIX Steelmaking Seminar - International of Associação Brasileira de Metalurgia e Materiais, Curitiba, Brazil, 2008
2 S. Alameddine and B. Bowman, “Electrical particularities of the meltdown in DC furnaces” 6th Electric Steel Conference, Düsseldorf, June 1999, p. 143-148 omit?